

Detection of in vivo Enzyme Activity with PARACEST MRI

B. Yoo¹, V. R. Sheth², C. A. Howison³, M. Douglas⁴, C. T. Pineda⁵, A. F. Baker⁶, and M. D. Pagel⁷

¹Biomedical Engineering, University of Arizona, Tucson, AZ, United States,

²Biomedical Engineering, Case Western Reserve University, Cleveland, OH, United States, ³Arizona Research Laboratories, University of Arizona, Tucson, AZ, United States, ⁴College of Medicine, University of Arizona, Tucson, AZ, United States, ⁵Arizona Cancer Center, University of Arizona, Tucson, AZ, United States, ⁶Hematology/Oncology, Arizona Cancer Center, University of

Arizona, Tucson, AZ, United States, ⁷Biomedical Engineering and Chemistry & Biochemistry, University of Arizona, Tucson, AZ, United States

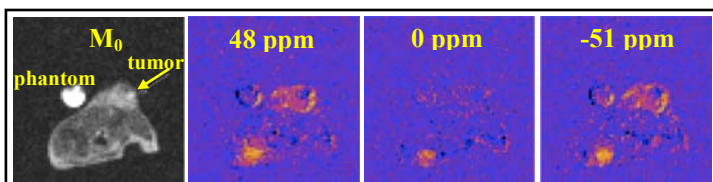


Figure 1. A CEST-FISP MR image before injection (M_0) and parametric CEST maps with saturation applied at 48, 0, and -51 ppm. The phantom did not contain the agent. The contrast in the bladder with 0 ppm saturation is attributed to B_0 inhomogeneity.

Introduction: We have pioneered the development and application of PARACEST MRI contrast agents that detect enzyme activities in vitro, including the detection of protease activity of urokinase Plasminogen Activator.¹⁻³ We have also developed methods for detecting PARACEST agents within mouse tumor models.⁴⁻⁶ This study combines these previous accomplishments to detect uPA enzyme activity within a mouse model of Capan-2 pancreatic cancer.

Methods: The PARACEST agent, ZGGR-(Tm-DOTA) was synthesized using our patented methods, and was shown to detect uPA enzyme activity in vitro.³ A "control" agent, Eu-DOTA-Gly₄ was also synthesized. A mouse model of a Capan-2 pancreatic tumor with an average size of 400 mm³ was used in this study. Each mouse was prepared for a MRI scan by anesthetizing with 2% isoflurane in O₂ carrier gas, a 27g catheter was installed in a tail vein, and respiration was monitored and core body temperature was maintained at 37 °C throughout the scan session. CEST-FISP MR images were acquired using a FISP sequence prepended with a 3-second saturation period applied at 10 μ T power and 1 ppm bandwidth.⁷ Selective saturation was applied at MR frequencies ranging from -80 to +80 ppm to acquire a MR CEST Spectroscopic Imaging (MR-CEST-SI) set, which required 100 seconds to acquire. A MR-CEST-SI set was acquired before injection, then 0.1 mL of a mixture of 100 mM of ZGGR-(Tm-DOTA) and 25 mM of Eu-DOTA-Gly₄ were injected i.v. within 1 minute, and then MR-CEST-SI sets were acquired for 18 minutes. Each MR-CEST-SI set was processed by manually selecting a region-of-interest for the tumor and bladder to create CEST spectra. Each spectrum was fitted with a single function of two Lorentzian lines initially centered at +51 ppm and -48 ppm and a super-Lorentzian line centered at 0 ppm, and the center frequency, width, and height of each line was allowed to change to best fit the experimental data. CEST effects were then determined by comparing the Lorentzian lines centered near +51 ppm and -48 ppm with the super-Lorentzian line at 0 ppm. In addition, parametric maps of the CEST effects, ($M_0 - M_S$)/ M_0 , were determined by subtracting the pre-injection image (M_0) from a post-injection image (M_S), and then normalizing with the pre-injection image. After the MRI scan session and before euthanasia, the mouse was allowed to recover to ensure that the PARACEST agent had no physiological effects. After each MRI scan session, uPA enzyme activity in ex vivo tumor tissue and blood plasma was confirmed with a fluorescence assay that used a ZGGR-AMC fluorophore.

Results: Parametric CEST maps showed that the agents accumulated in the tumor and bladder, but did not accumulate for sufficient CEST detection in the muscle (Figure 1). A representative CEST spectrum of a tumor at 5 minutes after injection showed 11.4% and 10.2% CEST effects from ZGGR-(Tm-DOTA) and Eu-DOTA-Gly₄ (Figure 2). The initial increase of the CEST effects from both agents was equivalent, indicating equivalent pharmacokinetics (Figure 3A). The CEST effect from the enzyme-responsive agent decreased more quickly than the control agent's CEST effect starting 6 minutes after injection, indicating that the enzyme-responsive agent was being cleaved by uPA (Figure 3B). The fluorescence assay confirmed that uPA enzyme activity was high in tumor tissue but not in blood plasma of this mouse model of Capan-2 pancreatic cancer.

Discussion: These results indicate that a comparison of enzyme-responsive and control PARACEST agents can detect enzyme activity within an in vivo tumor model.

References:

1. JACS, 2006, 128(43):14032-14033.
2. CMMI, 2007, 2:189-198.
3. Tet Letters, 2009, 50:4459-4462.
4. Magn Reson Med 2007, 58:1249-1256.
5. Molec Pharmaceutics, 2009, 6(5):1409-1416.
6. Acc Chem Res, 2009, 42(7):915-924.
7. Magn Reson Med, published on-line Oct 11, 2010.

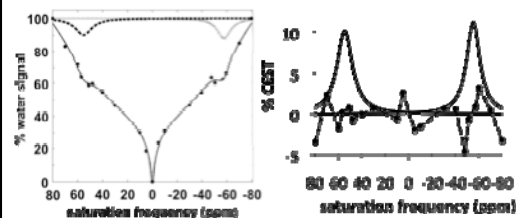


Figure 2. The CEST spectrum of the tumor at 5 minutes after injection, and the CEST effects measured from (super)-Lorentzian line fitting (residuals of the fitting shown as a dotted line).

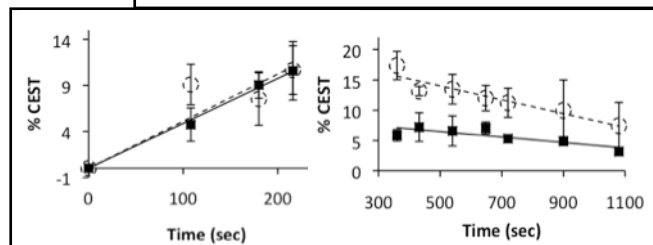


Figure 3. The CEST effects of the enzyme-responsive PARACEST agent (dotted circles, dotted line) and the control agent (filled squares, solid line) after co-injection.